HHS Public Access

Author manuscript

Cell Rep. Author manuscript; available in PMC 2015 November 14.

Published in final edited form as:

Cell Rep. 2015 November 10; 13(6): 1258–1271. doi:10.1016/j.celrep.2015.09.064.

Origin of a non-Clarke's column division of the dorsal spinocerebellar tract and the role of caudal proprioceptive neurons in motor function

Rachel Yuengert[1], **Kei Hori**[1,2], **Erin E. Kibodeaux**[1], **Jacob X. McClellan**[3], **Justin E. Morales**[3], **Teng-Wei P. Huang**[4,5], **Jeffrey L. Neul**[4,5,6], and **Helen C. Lai**[1,*]

[1] Department of Neuroscience, 5323 Harry Hines Blvd., UT Southwestern Medical Center at Dallas, Dallas, TX, 75390; USA

[2] Current position: Department of Biochemistry and Cellular Biology, National Institute of Neuroscience, NCNP, Tokyo 187-8502; Japan.

[3] Summer Undergraduate Research Fellowship (SURF) Program, 5323 Harry Hines Blvd., UT Southwestern Medical Center at Dallas, Dallas, TX 75390; USA

[4] Departments of Neurology, Molecular and Human Genetics, and Neuroscience, Program in Developmental Biology, One Baylor Plaza, Baylor College of Medicine, Houston, TX, 77030; USA

[5] Jan and Dan Duncan Neurological Research Institute, 1250 Moursund St., Houston, TX, 77030, USA

Summary

Proprioception, the sense of limb and body position, is essential for generating proper movement. Unconscious proprioceptive information travels through cerebellar-projecting neurons in the spinal cord and medulla. The progenitor domain defined by the basic helix-loop-helix (bHLH) transcription factor, ATOH1, has been implicated in forming these cerebellar-projecting neurons; however, their precise contribution to proprioceptive tracts and motor behavior is unknown. Significantly, we demonstrate that *Atoh1*-lineage neurons in the spinal cord reside outside Clarke's column (CC), a main contributor of neurons relaying hindlimb proprioception, despite giving rise to the anatomical and functional correlate of CC in the medulla, the external cuneate nucleus (ECu), which mediates forelimb proprioception. Elimination of caudal *Atoh1*-lineages results in mice with relatively normal locomotion, but unable to perform coordinated motor tasks. Altogether, we reveal that proprioceptive nuclei in the spinal cord and medulla develop from more than one progenitor source suggesting an avenue to uncover distinct proprioceptive functions.

[*]Corresponding Author: Helen C. Lai, 5323 Harry Hines Blvd., UT Southwestern Medical Center at Dallas, Dallas, TX 75390-9111, Helen.Lai@utsouthwestern.edu, (214) 648-4096 (tel), (214) 648-1801 (fax).

[6]Current address: Division of Child Neurology, Department of Neurosciences, Department of Pediatrics, 9500 Gilman Drive, UC San Diego, La Jolla CA 92093-0626

Author Contributions: R.Y., K.H., E.E.K., J.X.M., and J.E.M. performed experiments and analyzed data, T.P.H. and J.L.N. provided the *Hoxa4::Cre* mice before publication, H.C.L. conceived, performed, and analyzed the experiments and wrote the manuscript.

Abstract

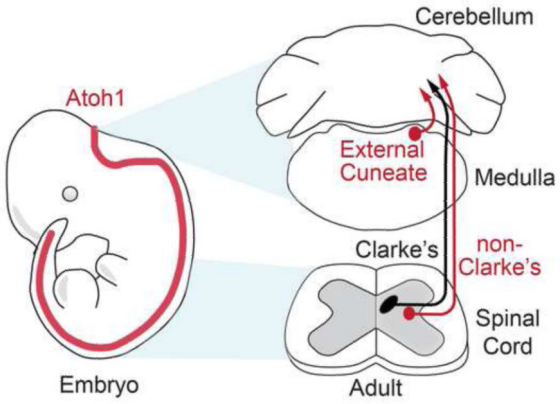

Introduction

Coordinated movement relies innately on proprioception, the sense of limb and body position (Sherrington, 1906). Humans who have lost their proprioceptive sense and mouse models that mimic this condition (Arber et al., 2000, Tourtellotte and Milbrandt, 1998, Cole, 1991, Akay et al., 2014) have great difficulty walking, indicating that proper proprioceptive sensory input is necessary for robust motor output. Unconscious proprioception is detected through primary sensory afferents that innervate muscle spindles and Golgi tendon organs sensing changes in muscle length and tension. These sensory neurons relay this information through the dorsal root ganglion (DRG) to cerebellar-projecting mossy fiber neurons either in the external cuneate nucleus (ECu) of the caudal medulla (the cuneocerebellar tract, CCT) for forelimb information or in the spinal cord through various spinocerebellar tracts (SCTs) for hindlimb information (Bosco and Poppele, 2001, Oscarsson, 1965). In particular, the dorsal spinocerebellar tract (DSCT) has been found to originate from several ipsilaterally-projecting neurons in the intermediate spinal cord (Matsushita and Hosoya, 1979, Edgley and Gallimore, 1988); the primary source being Clarke's column (CC)(dorsal nucleus of Clarke), a distinct set of neurons in the medial aspect of laminae VII in the thoracic to upper lumbar spinal cord (Oscarsson, 1965). CC has long been thought to be the hindlimb anatomical and functional correlate of the ECu (Oscarsson, 1965) and therefore, it was reasoned that they must develop from progenitor pools with a similar genetic signature. To test this hypothesis, we examined the lineage of the developmentally-defined population, *Atoh1* (Figure 1A).

The basic-helix-loop-helix transcription factor, ATOH1, in the developing neural tube, defines a progenitor domain generating proprioceptive pathway neurons in the hindbrain and spinal cord. In the hindbrain, *Atoh1*-lineage cells are a major source of neurons involved in proprioceptive-motor processing (cerebellar granule cell progenitors, deep cerebellar neurons, pontine nuclei, ECu, and lateral reticular nucleus (LRt))(Ben-Arie et al., 1997, Wang et al., 2005, Machold and Fishell, 2005, Rose et al., 2009, Landsberg et al., 2005). In the developing spinal cord, ATOH1 is transiently expressed in the highly restricted, dorsal-most, dorsal progenitor 1 (dP1) domain of the neural tube where it is required to specify the

dorsal interneuron 1 (dI1) population. This population has been implicated in forming various SCTs (Gowan et al., 2001, Bermingham et al., 2001, Sakai et al., 2012); however, detailed organization of *Atoh1*-lineage neurons in the postnatal spinal cord remains unknown.

Given ATOH1 in the rhombic lip gives rise to neurons in the ECu and elimination of *Atoh1* results in a reduction of DSCT-labeled axons (Bermingham et al., 2001, Rose et al., 2009), it has been presumed that *Atoh1*-lineage neurons must give rise to the CC portion of the DSCT. Unexpectedly, by following the lineage of *Atoh1* neurons, we discover that while they do indeed give rise to the ECu as has been previously published (Rose et al., 2009, Bermingham et al., 2001), they do not give rise to a majority of CC neurons in the spinal cord, the ECu functional correlate for the hindlimb. Instead, they cluster into a medial contralaterally-projecting and lateral ipsilaterally-projecting population in the intermediate spinal cord. We confirm that they receive proprioceptive input and propose that the lateral population makes non-CC sources of the DSCT (Matsushita and Hosoya, 1979, Edgley and Gallimore, 1988). In addition, we examine the behavioral consequences of eliminating caudal *Atoh1*-lineage proprioceptive neurons (ECu, LRt, and spinal cord), which has never been assessed due to the neonatal lethality of the *Atoh1* knockout (Ben-Arie et al., 1997). We discover that mice with a loss of caudal *Atoh1*-lineage neurons have relatively normal general motor behavior and pain sensation, but have clear deficits performing challenging motor tasks, uncovering a role for caudal *Atoh1*-lineage neurons in refined motor coordination. The reduced motor function in the hindlimb, but not complete ataxia, is consistent with the idea that only a subset of SCTs in the spinal cord was affected. Importantly, this work discovers that discrete proprioceptive pathways are distinguishable based on developmental molecular signature, which can be used to evaluate their contribution to motor behavior.

Results

Atoh1-lineage neurons are predominantly outside Clarke's column

We assessed the contribution of *Atoh1*-lineage neurons to proprioceptive centers in the caudal medulla and spinal cord by using the Cre-flox system. We chose to use the heterozygous $Atoh1^{Cre/+}$ knock-in mouse (Yang et al., 2010) because transgenes using the *Atoh1* autoregulatory enhancer demonstrated ectopic expression in the nervous system (Lumpkin et al., 2003, Matei et al., 2005, H.C.L. unpublished observations). While it is possible that the $Atoh1^{Cre/+}$ knock-in mice may have half the gene dosage of wild type mice, there is evidence that this will have minimal effect on reporter output. In particular, *Atoh1* positively autoregulates its own expression (Helms et al., 2000) and heterozygous $Atoh1^{LacZ/+}$ knock-in mice have been shown to accurately recapitulate *Atoh1* expression (Ben-Arie et al., 2000, Bermingham et al., 2001). In addition, *in situ* hybridization of *Cre* mRNA in $Atoh1^{Cre/+}$ mice at E10.5 mimics *Atoh1* expression (Figure S1A, arrows) and analysis of *Atoh1*-lineage neurons at E11.5 demonstrates that the $Atoh1^{Cre/+}$ mouse line reliably labels dI1 neurons (LHX2/9+, Figure S1B, arrows) and not neighboring neurons (LHX1/5+, Figure S1B, arrowheads).

By crossing the *Atoh1*$^{Cre/+}$ knock-in mice to Cre-dependent reporter mice expressing TOM (Ai14, *R26R*$^{LSL\text{-}tdTomato}$)(Madisen et al., 2010) or GFP (*R26R*$^{LSL\text{-}GFP}$)(Miyoshi et al., 2010)), we were able to follow the *Atoh1*-lineage and determine their contribution to proprioceptive centers using vesicular glutamate transporter 1, *Vglut1*, as a marker for proprioceptive nuclei. Notably, *Vglut1*, marks cerebellar-projecting neurons in the ECu, LRt, and CC (Figure 1B and 1D)(Malet et al., 2013, Llewellyn-Smith et al., 2007). *Atoh1*-lineage cells (GFP+) in the lower medulla (ECu and LRt regions) are almost entirely *Vglut1*+ (simultaneous *in situ* hybridization (ISH) and immunohistochemistry (IHC))(Gray, 2013) (Figure 1B-C, 86.7 ± 1.3% for ECu and 91.8 ± 0.2% for LRt). These ECu neurons are likely to express vesicular glutamate transporter 2, *Vglut2*, as well (Hisano et al., 2002). Strikingly, a majority (>99%) of the *Atoh1*-lineage neurons in the spinal cord do not express the CC marker, *Vglut1* (Figure 1D, 0.5 ± 0.1%). However, *Atoh1*-lineage neurons in the spinal cord are glutamatergic (*Vglut2*+, Figure 1E, 82.2 ± 2.2%). In addition, a majority of *Atoh1*-lineage cells expressed the neuronal marker, NeuN (95.5 ± 0.9%) and 4.2 ± 0.1% of the NeuN+ cells in the spinal cord are *Atoh1*-lineage (counts from 12 representative sections from T1-13 per n=2, P14 spinal cords from 2 litters), while none expressed glial markers OLIG2 and SOX2.

CC can be identified by injection of retrograde tracers into the cerebellum (Matsushita and Hosoya, 1979). To corroborate that *Atoh1*-lineage neurons do not form a majority of CC, we stereotaxically injected a retrograde tracer, cholera toxin subunit B (CTB) conjugated to Alexa 488, into adult mouse cerebella (Figure 2A). When the CTB tracer was injected into the vermis at folia IV-VI (Figure 4A, labeling approximately a 1 mm × 1.5 mm × 1.5 mm volume), neurons known to project to the cerebellum from the medulla (ECu, LRt, and inferior olive (IO)) took up the tracer (diagrammed in Figure 2B) verifying our retrograde labeling technique. In particular, *Atoh1*-lineage neurons in the ECu and LRt (Figure 2B'-B'', 3-5 months old, n=3 from 3 litters) were retrogradely labeled confirming previously published backlabeling of the ECu *Atoh1*-lineage neurons at P0 (Bermingham et al., 2001). However, while retrograde labeling of CTB from the cerebellum labels CC (Figure 2C), we found only 10.5 ± 0.08% of the CTB-labeled CC neurons are *Atoh1*-lineage (Figure 2C'). Therefore, a small percentage of CC neurons labeled by anatomical tracing are *Atoh1*-lineage.

Lastly, CC can also be marked by expression of glial derived neurotrophic factor (*Gdnf*) (Hantman and Jessell, 2010). In support of the hypothesis that *Atoh1*-lineage neurons do not form a majority of CC, we found that *Gdnf* expression is not significantly different in *Atoh1* wild type (*Atoh1*$^{+/+}$) versus heterozygous (*Atoh1*$^{+/\Delta}$) versus null (*Atoh1* $^{\Delta/\Delta}$) mice (Figure 2D-E)(# *Gdnf* cells, 45 ± 5, 36 ± 5, 43 ± 2, respectively). Note that we were unable to use the CC marker, *Vglut1*, since it is not yet expressed at E18.5, the stage at which we must assay expression, since *Atoh1* null mice are neonatal lethal. Altogether, we find that *Atoh1*-lineage neurons form the ECu and LRt in the medulla, but not a majority of CC neurons in the spinal cord. However, the possibility remains that CC may form from an early-born *Atoh1*-lineage population that does not require *Atoh1*.

Atoh1-lineage neurons form a medial contralaterally-projecting and lateral ipsilaterally-projecting population

We examined the distribution and axonal projections of mature *Atoh1*-lineage neurons. We found that *Atoh1*-lineage (TOM+) cells in the spinal cord form two spatially distinct populations in the intermediate areas throughout the rostral-caudal (r-c) axis (Figure 3A-B’’’, Figure S2). *Atoh1*-lineage cells migrate extensively from their dorsal-most location during development (Figure 1A) and settle primarily in lamina V through VII, with a few cells found in other laminae, including the intermediolateral (IML), lamina VIII, and IX (Figure 3A-A’’, Figure S2A’’’-F’’’). Laminae were delineated using NeuroTrace, a fluorescent Nissl stain and the Christopher and Dana Reeve atlas (Watson et al., 2009) as a guide. In addition, *Atoh1*-lineage neurons cluster into a smaller medial (M) population and a larger lateral (L) population throughout the r-c axis (Figure 3B-B’’’, Figure S2A’-F’’).

Furthermore, we investigated the axonal projections of the M and L populations both developmentally and in maturity. Using a Cre-inducible strategy with a membrane-GFP reporter (*Atoh1::CreER*^{T2};*Tau*$^{LSL\text{-}mGFP}$)(Machold and Fishell, 2005, Hippenmeyer et al., 2005), we found that both the M and L *Atoh1*-lineage populations are born between E9.5 and E11.5 (Figure 3C). By E13.5, the contralateral axons of the M population are seen in the ventral funiculus (Figure 3C, pink ovals) and the ipsilateral axons of the L population are seen in the lateral funiculus (Figure 3C, blue ovals), consistent with the dI1c and dI1i populations, previously described for the development of dI1 neurons (Miesegaes et al., 2009, Wilson et al., 2008, Imondi et al., 2007, Ding et al., 2012). However, to examine if this axonal pattern is maintained in maturity, individual cells from acute spinal cord slices (T9-L3, P12-P15) were filled and stained for biocytin. As shown in an example L cell, axons could be clearly distinguished from dendrites as long, thin processes that did not contain spines (Figure 3D, arrowheads). Shown on a polar coordinate graph, the dendrites for the M population extended both laterally and ventrally (Figure 3E, blue), while the axons projected contralaterally (Figure 3E, red, n=6 cells). For the L population, the dendrites extended medially (Figure 3F, blue) and the axons extended mainly to the ipsilateral lateral funiculus with some collateral axons projecting ventrally in the spinal cord (Figure 3F, red, n=17 cells). Many of the *Atoh1*-lineage neurons had a unique morphology with an axon branching from a primary neurite as opposed to branching from the soma (6 out of 6 M neurons, 13 out of 17 L neurons)(Figure 3D, arrow). In total, the medial contralaterally-projecting and lateral ipsilaterally-projecting populations seen during development (dI1c and dI1i) are maintained in maturity (defined here as M and L, respectively).

Atoh1-lineage cells receive proprioceptive information

Since a majority of *Atoh1*-lineage neurons do not reside in CC, we wanted to determine if they might receive proprioceptive information. We directly visualized proprioceptive synapses on M TOM+ cells by immunostaining proprioceptive afferents with parvalbumin (PV+)(Arber et al., 2000) and presynaptic terminals with VGLUT1+ (Hantman and Jessell, 2010)(Figure 4A-A’). Note that we are detecting VGLUT1 protein at presynaptic terminals from the proprioceptive sensory neurons as opposed to *Vglut1* mRNA expression in the cell bodies of CC neurons in the spinal cord. However, we were unable to directly visualize synaptic contacts on the L population.

To examine if both the M and L *Atoh1*-lineage populations could receive PV+ proprioceptive inputs, we took an electrophysiological approach by performing whole cell patch clamp in acute spinal cord slices. We expressed TOM *(R26R$^{LSL\text{-}tdTomato}$)* and EYFP-fused channelrhodopsin (Ai32, *R26R$^{LSL\text{-}ChR2(H134R)\text{-}EYFP}$*, *ChR2-EYFP*)(Madisen et al., 2012) in both the PV+ afferents (*Pv$^{IRES\text{-}Cre/+}$*) and the *Atoh1*-lineage neurons *(Atoh1$^{Cre/+}$)* (Figure 4B). Since PV+ afferents are spatially distinct from *Atoh1*-lineage neurons, we were able to get selective activation of *ChR2-EYFP* in the PV+ afferents by illuminating focal blue light specifically on the dorsal funiculus while recording from an *Atoh1*-lineage neuron to determine synaptic connectivity. While *ChR2-EYFP* and TOM were substantially expressed in the PV+ afferents, the *Atoh1*-lineage neurons expressed considerably higher levels of TOM, which was used to visualize neurons for whole-cell patching (Figure 4C). In addition, we verified that the *Pv$^{IRES\text{-}Cre/+}$* reliably labeled sensory PV+ neurons (Figure 4D).

When focal blue light (10 ms, 100-250 μm diameter) was directed at a M TOM+ cell, a direct inward current was seen (Figure 4E, F). However, when blue light was directed to the dorsal funiculus on the ipsilateral side of the cell being recorded, we saw a reproducible excitatory postsynaptic current (EPSC)(Figure 4E', F') that was eliminated by application of the AMPA blocker, DNQX, and restored upon washout (Figure 4E''-F'''). No EPSC was seen when blue light illuminated the contralateral dorsal funiculus (Figure 4E'''', F''''). Similar results were obtained for a L TOM+ cell (Figure 4G-H'). As expected, some recorded cells did not have a synaptic response to blue light stimulation of the dorsal funiculus (Figure 4I-I'), indicating they were either not connected or that their connections were severed due to the acute slice model. In total, 3 out of 12 M cells and 5 out of 11 L cells recorded resulted in an EPSC in the *Atoh1*-lineage neuron in this paradigm. Furthermore, repeated stimulation (3-4 times at 30 sec intervals) of a single cell showed that the EPSC latency (start time of blue light illumination to start of EPSC) for some individual cells was highly reproducible (Figure 4K). However, we could not unambiguously determine if these were monosynaptic connections since we could not achieve the high firing rates necessary to resolve this using jitter analysis (Doyle and Andresen, 2001) due to run down of the channelrhodopsin-activated EPSC upon high frequency stimulation. Biocytin staining of a L *Atoh1*-lineage neuron shows that some dendrites project toward the PV+ sensory afferents (Figure 4L) to receive proprioceptive inputs.

As a control, we could not detect *Atoh1*-lineage neurons within the spinal cord making synaptic contacts onto other *Atoh1*-lineage neurons. We expressed TOM and *ChR2-EYFP* only in the *Atoh1*-lineage (Atoh1$^{Cre/+}$; R26R$^{LSL\text{-}tdTomato}$, R26R$^{LSL\text{-}ChR2(H134R)\text{-}EYFP}$) and did not see any EPSCs when the ipsilateral dorsal funiculus was illuminated (Figure 4J-J'), which is expected since *Atoh1* is not expressed in the DRG (n=8 for M and n=8 for L), or when the entire slice was illuminated (data not shown). In addition, while PV+ neurons can be detected in the adult mouse spinal cord (Fu et al., 2012), there are very few labeled at these early stages (P12-P15) and we were unable to patch any cells in control Pv$^{IRES\text{-}Cre/+}$; R26R$^{LSL\text{-}tdTomato}$, R26R$^{LSL\text{-}ChR2(H134R)\text{-}EYFP}$ slices (n=16 slices) indicating that it is unlikely that we have patched *Pv$^{IRES\text{-}Cre/+}$* cells in our studies. Altogether, a portion of *Atoh1*-lineage neurons in both the M and L populations receive PV+ input suggesting these

form spinocerebellar neurons, and in particular, the ipsilaterally-projecting L population comprises a non-CC source of the DSCT.

Generation of Atoh1 conditional knockout mice

In addition to spinocerebellar neurons in the spinal cord, *Atoh1*-lineage cells are a major source of hindbrain neurons involved in proprioceptive-motor control including cerebellar granule cells, deep cerebellar neurons, pontine nuclei, ECu, and LRt cells. The function of these caudal, non-cerebellar *Atoh1*-lineage neurons on proprioceptive-motor behavior has never been examined as the *Atoh1* knockout mouse is neonatal lethal, precluding an examination of motor behaviors (Ben-Arie et al., 1997). Therefore, we pursued a conditional knockout strategy to eliminate *Atoh1*-lineage neurons in caudal regions of the neural tube, leaving structures such as the cerebellum, pontine nucleus, and essential breathing centers in the hindbrain intact.

We used a previously published *Hoxa4::Cre* transgenic mouse that expresses *Cre* in regions caudal to rhombomere 6/7 throughout embryogenesis (Figure 5B-D) (Huang et al., 2012). We found that the *Cre* was expressed in the *Atoh1* domain as early as E9.5 when *Atoh1* is first expressed (Figure 5B-B’’)(Ben-Arie et al., 1996). We crossed *Hoxa4::Cre;Atoh1*$^{\Delta/+}$ mice, which contain an *Atoh1* null allele to floxed *Atoh1* mice (*Atoh1*$^{f/f}$) (Figure 5A) (Shroyer et al., 2007), to determine the contribution of caudal *Atoh1*-lineage cells to proprioception. The three “control” genotypes (*Atoh1*$^{f/+}$, *Hoxa4::Cre;Atoh1*$^{f/+}$, and *Atoh1*$^{\Delta/f}$) were treated as equal since no difference was detected between these mice in any of the behavioral assays. The *Hoxa4::Cre;Atoh1*$^{\Delta/f}$ genotype is henceforth called “*Atoh1* CKO.”

We first verified that *Atoh1* was efficiently knocked out specifically in the caudal neural tube through detection of *Atoh1* mRNA, *Atoh1*-lineage markers, and an Atoh1-GFP BAC reporter strain (*Atoh1BAC::GFP*)(Raft et al., 2007, Lai et al., 2011) where GFP is controlled by *Atoh1* regulatory elements. We found that *Vglut1*+ cells were significantly reduced in the ECu, LRt, and total caudal medulla with 51 ± 9%, 31 ± 3%, and 41 ± 5% of *Vglut1*+ cells remaining in these areas, respectively (Figure 5E-F). We estimate that 80-90% of neurons in the ECu and LRt in the medulla are *Atoh1*-lineage (H.C.L. unpublished data). Thus, the reduction in *Vglut1*+ cells is interpreted as a mosaic loss of *Atoh1* expression at the rostral end of *Hoxa4::Cre* expression. At embryonic stage E11.5, *Atoh1* (mRNA), *Atoh1*-lineage markers (*Lhx2* and *Barhl2* mRNA)(Gowan et al., 2001, Bermingham et al., 2001, Saba et al., 2005), and the GFP reporter were clearly eliminated caudal to rhombic lip regions while these markers in the rhombic lip were still intact (Figure 5G-Q’) (at least n=3 embryos from 2 litters checked for control and *Atoh1* CKO genotypes). These experiments verify that *Atoh1* and the neuronal markers for lineages requiring ATOH1 were completely eliminated in the developing spinal cord and substantially reduced in the lower medulla.

To ensure that the loss of ATOH1 neurons in the caudal neural tube did not cause secondary effects on proprioceptive pathways and motor neurons that might alternatively explain a motor phenotype, we confirmed that Clarke’s column (*Vglut1*+), the distribution of PV+ proprioceptive afferents, and HB9+ motor neurons were unchanged in the *Atoh1* CKO mice throughout the rostral-caudal axis (Figure 6A-C’’). Lastly, the cerebellar morphology in

medial (Figure 6D-D') and lateral (Figure 6E-E') areas was grossly normal (n=2 each from 2 litters, control and *Atoh1* CKO, 9-10 months old).

Finally, when *Atoh1* is lost, dI1 lineage cells have been reported to transfate to neighboring populations: *Neurog1*-lineage, roof plate, or a Sox9+ lineage at embryonic stages (Gowan et al., 2001, Bermingham et al., 2001, Miesegaes et al., 2009). However, it is not known whether these transfated cells are maintained into adult stages. We were able to detect a subset of *Atoh1*-lineage neurons that transfate to a FOXP2+PAX2− population that are presumably *Neurog1*-lineage neurons (Prasad et al., 2008). By following the cells that would have become *Atoh1*-lineage in the *Atoh1* null ($Atoh1^{Cre/\Delta}$; $R26R^{LSL\text{-}tdTomato}$), we found that some TOM+ cells are FOXP2+PAX2− (Figure 6F', arrows) compared to none in heterozygous controls (Figure 6F, $Atoh1^{Cre}$; $R26R^{LSL\text{-}tdTomato}$). However, since *Atoh1* is positively autoregulatory (Helms et al., 2000), the TOM+ cells in the *Atoh1* null capture only a subset of potentially transfated neurons. Therefore, we analyzed the percentage of FOXP2+PAX2− cells out of total FOXP2+ cells in *Atoh1* heterozygous versus null mice and found no significant difference at E18.5 (Figure 6F'', 58 ± 1% vs. 61 ± 1%, respectively). This suggests that homeostatic mechanisms may come into play to keep this subset of *Neurog1*-lineage neurons in check and that these particular transfated neurons may not significantly influence the phenotype. Furthermore, the generation of transfated neurons does not extend to the ISLET1+ dI3 population which was unaffected in heterozygous ($Atoh1^{+/\Delta}$) versus null ($Atoh1^{\Delta/\Delta}$) mice (378 ± 25 vs. 361 ± 17 cells, respectively, p~0.6, mean ± SEM, counts from 4 representative sections per n=3 embryos from 1 litter). Lastly, no difference in the total number of NeuN+ cells was detected in control versus *Atoh1* CKO mice at P10 (14468 ± 314 vs. 14041 ± 503 NeuN+ cells, respectively, p ~ 0.5, mean ± SEM, counts from 12 representative T1-13 sections for n=3 from 3 litters). However, only 4.2% of the NeuN+ cells in the thoracic spinal cord are *Atoh1*-lineage and the error in counting was 2-4%, so a difference in total number of NeuN+ cells in the spinal cord due to the *Atoh1* CKO would be undetectable.

Caudal Atoh1 conditional knockout mice have marked balance and motor coordination defects when challenged

Strikingly, the *Atoh1* CKO mice were grossly normal, even though *Atoh1*-lineage neurons were decreased in the major proprioceptive centers, ECu and LRt, and knocked out in areas caudal to these. They had similar mass, length, and width compared to control at 9-13 weeks of age when most of the behavior tests were performed (Figure 7A-C). A neurological exam found that their eyeblink, visual placing, vibrissae orientation, negative geotaxis, postural, and righting reflexes were normal (data not shown)(Lake, 2005). When mice were placed in a novel cage for five minutes (activity test), the *Atoh1* CKO mice froze, reared, and groomed the same number of times as control mice (Figure S3A-C). However, during the activity test, the *Atoh1* CKO mice exhibited odd stereotypical behaviors making them readily distinguishable from control mice. When freezing, the *Atoh1* CKO mice repeatedly retracted one forepaw as opposed to having all four paws on the ground (Figure 7D). In addition, their forepaws would retract during unsupported rearing (Figure 7E) and they would "reach" for the wall during supported rearing (Figure 7F)(See Movies S1 and S2). The *Atoh1* CKO mice also had a noticeable hunched posture, bobbing behavior, and elevated step in their

hindlimbs. While postural and righting reflexes were intact and *Atoh1*-lineage neurons rostral to the lower medulla, including vestibular nuclei, should have been unaffected in the *Atoh1* CKO mice, we cannot exclude secondary effects to the vestibulospinal pathways that could account for these balance and postural defects. The *Atoh1* CKO mice were more active and moved more distance in an open field (Figure S3F), which may lead to their eventual decreased mass by age 23-27 weeks (Figure 7A). When placed in an open field, the mice exhibited similar anxiety compared to control (Figures S3E, center). Conspicuously, the *Atoh1* CKO mice stayed slightly further away from the periphery (5 cm versus 10 cm from the periphery, Figure S3D).

To get a better indication of the motor impairment in *Atoh1* CKO mice, we evaluated the gait of these mice using the DigiGait system allowing us to quantitate several parameters regarding their walking behavior. *Atoh1* CKO mice had a noticeably shorter stride reflected in a shorter stride time and increased stride frequency (Figure 7G-I). This was mostly due to a decreased stance time for the forelimbs (FL) and a combined decreased time for stance and swing phases in the hindlimbs (HL)(Figure 7H). In addition, the paw area at peak stance was significantly decreased in the HL (Figure 7J) supporting the observation from the activity test that the *Atoh1* CKO mice were elevated on their HL. Notably, the angle of the paws was splayed outward for both FL and HL (Figure 7K). However, the gait of *Atoh1* CKO mice was relatively normal with no difference in stance width (Figure 7L) and no apparent ataxia (Figure 7M). Furthermore, indices that reflect normal walking such as gait symmetry (control vs. *Atoh1* CKO: 1.00 ± 0.01 vs 1.01 ± 0.05) and paw area variability at peak stance ((FL) 0.034 ± 0.017 vs. 0.035 ± 0.016 cm^2); (HL) 0.052 ± 0.025 vs. 0.049 ± 0.017 cm^2) were not significantly different. Overall, these data suggest that *Atoh1* CKO mice had only a handful of defects in their gait.

The most obvious deficits in *Atoh1* CKO mice were observed when they were challenged with balance or coordination tests. They performed reasonably well on a large balance beam (18 mm wide), taking a similar time to cross despite more foot slips (Figure 7N). However, as the beam narrowed (9 mm and 5 mm), they took much longer to cross and slipped significantly more (Figure 7N). When crossing a horizontal ladder, the *Atoh1* CKO mice had noticeable defects in proper paw positioning. The *Atoh1* CKO mice would often strike the ladder rung with their heel or entirely miss or slip off the rung rather than grasp the rung with their toes as control mice did. These inaccuracies resulted in a decreased “quality step” score and increased ratio of missteps (Figure 7O, Movies S3 and S4). On an accelerating rotarod, the *Atoh1* CKO mice immediately fell (Figure 7P). In part, these deficits might be due to a lack of gripping ability (Figure S3G-I). However, the phenotype was specific to balance and motor coordination, as thermal and nociceptive responses appeared normal (Figure 7Q-S).

Discussion

Proprioceptive sensory input is critical for generating proper motor output. Humans and animal models that have lost their proprioceptive primary afferent input result in an inability to walk or severe ataxia. In this study, we interrogate proprioceptive neurons at the level of the caudal medulla and spinal cord to understand their contribution to proprioceptive circuits

and behavior. Unexpectedly, we discovered that even though the ECu and CC have long been thought to be functional and anatomical correlates, they derive from developmental lineages with different molecular signatures. This suggests either a convergence of progenitor domains with different molecular signatures to a similar function or perhaps common functions between *Atoh1*-lineage non-CC and ECu neurons that have yet to be identified. In addition, we find that by removing *Atoh1* in caudal regions of the developing neural tube, the mice are able to walk relatively normally, but have deficits when challenged with highly coordinated motor tasks. Significantly, this study provides evidence that proprioceptive relay neurons at the level of the spinal cord are genetically distinct (CC vs non-CC) and demonstrates how identification and elimination of molecularly discrete populations can begin to uncover characteristic differences in proprioceptive processing.

Atoh1-lineage neurons form subsets of SCTs

Previous work has implicated *Atoh1*-lineage neurons in forming SCTs and shown that both the contralaterally- and ipsilaterally-projecting populations during embryogenesis project to the cerebellum (Sakai et al., 2012, Bermingham et al., 2001). However, precisely how they contribute to SCTs in adulthood was unknown. We show here that *Atoh1*-lineage neurons migrate quite extensively from their dorsal-most birth location to form a M and L population in the intermediate spinal cord, a majority of which do not reside in CC, a main source of the DSCT. In addition, the contralaterally-projecting M *Atoh1*-lineage is not located near spinal border cells in the lateral lumbar regions of the spinal cord that contribute to the contralaterally- projecting ventral spinocerebellar tract (VSCT). Therefore, our work combined with earlier evidence suggests that *Atoh1*-lineage neurons contribute to novel sources of the DSCT and VSCT that reside in deep laminae (Edgley and Gallimore, 1988, Matsushita and Hosoya, 1979). In particular, the ipsilaterally-projecting L *Atoh1*-lineage neurons closely match previously described ipsilaterally-projecting sets of SCTs in cats and rats: cervical (named medial lamina VI-SCT, central lamina VII-SCT), lower cervical to lumbar (lamina V-SCT or dorsal horn SCT (dhSCT)), and lumbar (medial lamina VI-SCT) (Matsushita and Hosoya, 1979, Matsushita et al., 1979, Edgley and Gallimore, 1988, Edgley and Jankowska, 1988). Furthermore, the contralaterally-projecting M *Atoh1*-lineage population most closely corresponds to contralaterally-projecting SCTs in the cervical and lumbar regions in rat and cat (named central cervical nucleus (CCN)-SCT and medial lamina VII-SCT, respectively). Altogether, *Atoh1*- lineage neurons form subsets of the DSCT and VSCT that previously could not be isolated from the entire tract.

Furthermore, the cerebellum is likely not the only target of *Atoh1*-lineage neurons. Experiments in chick have shown that dI1 neurons also terminate in the developing pons or medulla (Avraham et al., 2009, Sakai et al., 2012). In addition, axon collaterals from biocytin tracing can be seen in the L population projecting ventrally and medially (Figure 3F, axon polar coordinates 230°) suggesting these neurons might be both projection neurons and spinal interneurons.

Information processing of Atoh1-lineage neurons

Based on the location of the L *Atoh1*-lineage neurons, it is possible that they contribute to what is termed the “exteroceptive”, relating to the perception of external stimuli, division of

the DSCT (Oscarsson, 1965, Mann, 1971). The “proprioceptive” division of the DSCT in CC receives mainly muscle spindle (Ia and weak II) and Golgi tendon organ (Ib) inputs (Eccles et al., 1961). However, electrophysiological recordings of populations contributing to the DSCT, but located lateral and/or caudal to Clarke’s column, similar to where *Atoh1*-lineage neurons reside, have shown that these neurons can receive both proprioceptive and cutaneous input (Tapper et al., 1975, Randic et al., 1976, Edgley and Jankowska, 1988) suggesting they contribute to the exteroceptive division. In addition, the ECu has been reported to have both an exteroceptive and proprioceptive subdivision similar to the spinal cord; however, the exteroceptive inputs to the ECu are mostly polysynaptic (Oscarsson, 1965) and the exact location of the exteroceptive division is a matter of some debate (Cooke et al., 1971). Given that both the ECu and the L neurons in the spinal cord both derive from the *Atoh1*-lineage, it will be interesting to explore any functional commonalities of these neurons.

While PV labels mostly proprioceptive afferents, less than 10% of PV+ sensory neurons are low-threshold mechanoreceptors involved in detection of vibration, hair follicle deflection, and skin movement, but not light touch (Abraira and Ginty, 2013, de Nooij et al., 2013). Therefore, in our slice recording preparations, we may have detected some cutaneous inputs onto spinal cord *Atoh1*-lineage neurons. Interestingly, mice with their *Atoh1*-lineage light touch Merkel cells eliminated perform normally on rotarod and wire hang tasks (Maricich et al., 2012) indicating these cells do not contribute to a motor phenotype. Together, these data suggest that specific low-threshold mechanoreceptor and proprioceptive information may be integrated at the level of *Atoh1*-lineage neurons in the spinal cord and be critical for appropriate coordinated motor function.

Consequences of deleting caudal Atoh1-lineage neurons

Studies that have altered neurons in proprioceptive/motor pathways have obvious motor deficits. Elimination of primary proprioceptive afferents, knockouts of neurons involved in the central pattern generator in the ventral spinal cord (Lanuza et al., 2004, Talpalar et al., 2013, Crone et al., 2008), and complete knockout of *Barhl2*, a transcription factor that is a downstream target of ATOH1 (Ding et al., 2012), produce mice with abnormal left-right alternation or clear ataxia. Complete elimination of SCTs would have predicted a severe ataxic motor phenotype in the hindlimbs. However, the *Atoh1* CKO mice are not ataxic, but have defects in coordinated motor behavior, consistent with the idea that spinal cord *Atoh1*-lineage neurons are required for subsets of proprioceptive information relayed through SCTs.

The behavior seen in *Atoh1* CKO mice can be attributed to different proprioceptive nuclei (ECu, LRt, and various SCTs in the spinal cord) and potentially *Atoh1*-lineage neurons in the ventral spinal cord (Figure 3B’, black dots) that have not yet been characterized. Importantly, *Atoh1*-lineage cells do not form neurons in the inferior olive, the major source of climbing fibers to the cerebellum, and therefore do not contribute to the motor phenotype in this way (Landsberg et al., 2005, Yamada et al., 2007, Wang et al., 2005). The ECu relays forelimb proprioceptive information and the LRt integrates spinal cord information regarding posture and locomotion (Alstermark and Ekerot, 2013, Cooke et al., 1971).

Therefore, the forelimb phenotypes are likely due to *Atoh1*-lineage neurons reduced in the ECu and LRt. Pharmacological ablation of the LRt in cats show defects in posture and reflex movements (Santarcangelo et al., 1981), consistent with a subset of behaviors seen in the *Atoh1* CKO mice (i.e. hunched posture). Furthermore, hindlimb defects can be attributed to both *Atoh1*-lineage neurons in the LRt and spinal cord. Interestingly, a recent report studying the behavior of mice with degenerate muscle spindle sensory neurons showed similar motor defects as the *Atoh1* CKO mice (i.e. inability to perform the ladder rung test) (Akay et al., 2014). Differences in how the motor behavior was analyzed preclude a direct quantitative comparison between these two studies; however, it necessitates future experiments to delineate precisely how muscle spindle and Golgi tendon organ information integrate at the level of *Atoh1*-lineage and CC spinal cord neurons.

Future experiments acutely disrupting the function of *Atoh1*-lineage neurons in the adult medulla or spinal cord will help clarify the contribution of more rostral or caudal neurons to the observed forelimb and hindlimb phenotypes. In addition, the discovery that *Atoh1*-lineage neurons form a non-CC subset of the DSCT leaves open the question as to the developmental source of CC. More broadly, however, the question arises whether a progenitor source with a common genetic signature forms neurons with similar function.

Experimental Procedures

Experimental Animals—*Atoh1*$^{Cre/+}$ knock-in (Yang et al., 2010), *Atoh1::CreER*^{T2} transgenic (Machold and Fishell, 2005), *R26R-loxP-STOP-loxP-LacZ (R26R*$^{LSL\text{-}LacZ}$*)* (Soriano, 1999), *R26R-loxP-STOP-loxP-tdTomato* (*R26R*$^{LSL\text{-}tdTomato}$ or TOM, Ai14, Allen Brain Atlas) (Madisen et al., 2010), *R26R-CAG- loxP-STOP-loxP-EGFP* (*R26R*$^{LSL\text{-}EGFP}$, named *RCE::loxP* in Miyoshi et al., 2010) (Miyoshi et al., 2010), *Tau*$^{LSL\text{-}mGFP}$ (Hippenmeyer et al., 2005), *Atoh1BAC::GFP* transgenic (Raft et al., 2007, Lai et al., 2011), *Atoh1*$^{\Delta/+}$ (Ben-Arie et al., 1997), *Atoh1*$^{F/F}$ (Shroyer et al., 2007), *Hoxa4::Cre* (Huang et al., 2012), *R26R-LSL-ChR2(H134R)-EYFP-WPRE* (*R26R*$^{LSL\text{-}ChR2(H134R)\text{-}EYFP}$, abbreviated *ChR2-EYFP*, Ai32, Allen Brain Atlas)(Madisen et al., 2012), and *Pv*$^{IRES\text{-}Cre/+}$ (Hippenmeyer et al., 2005), transgenic mice were previously published. Embryos were timed as E0.5 on the day a vaginal plug was detected. The age of pups was counted as P0 on the day of birth. Both male and female mixed strain mice (minimally C57BL/6J, 129S6, 129/Ola, and ICR) were used. All animal experiments were approved by the Institutional Animal Care and Use Committee at UT Southwestern.

See **Supplemental Experimental Procedures** for details regarding the *Atoh1*$^{Cre/+}$; *R26R*$^{LSL\text{-}tdTomato}$ animals, Tissue Preparation, Immunohistochemistry (IHC), in situ hybridization (ISH), Microscopy, Electrophysiology, Biocytin staining, Stereotaxic Injections, and full description of Behavioral Tests.

Supplementary Material

Refer to Web version on PubMed Central for supplementary material.

Acknowledgements

We thank L. Gan for the *Atoh1*$^{Cre/+}$ mice, G. Fishell for the *Atoh1::CreER*^{T2} transgenic mice, S. Arber for the *Tau*$^{LSL\text{-}mGFP}$ mice, T. Jessell for the rabbit anti-LHX2/9 and ISL1/2 antibodies, *Lhx2* and *Gdnf* ISH probe, S. Pfaff for the rabbit anti-HB9 antibody, T. Saito for the *Barhl2* ISH probe, and R. Seal for the *Vglut1* ISH probe. We are eternally indebted to Dr. Jane E. Johnson for her unwavering support and continuing partnership. We thank several UTSW Core facilities for their time and essential expertise: S. Birnbaum and L. Peca-Behavior Core, E. Plautz and S. Rovnisky-Neuro-Models Core, I. Bowen-Quantitative Morphology Core, J. Shelton-Histology Core, and D. Ramirez-Whole Brain Imaging Facility. Thanks to H. Zoghbi for helpful direction, P. Gray for invaluable discussions, K. Huber and J. Gibson for guidance and resources, and T. Vue and E. Kim for critical reading of the manuscript. Many thanks to J. Wilkerson, D. Crawford, J. Fan, M. Borromeo, and T. Savage, and members of the Huber, Gibson, and Johnson labs for technical assistance. This work was supported by the Sara and Frank McKnight Fellow program to H.C.L and NIH/NICHD HD062553 to J.L.N. The authors declare no competing financial interests.

References

ABRAIRA VE, GINTY DD. The sensory neurons of touch. Neuron. 2013; 79:618–39. [PubMed: 23972592]

AKAY T, TOURTELLOTTE WG, ARBER S, JESSELL TM. Degradation of mouse locomotor pattern in the absence of proprioceptive sensory feedback. Proc Natl Acad Sci U S A. 2014; 111:16877–82. [PubMed: 25389309]

ALSTERMARK B, EKEROT CF. The lateral reticular nucleus: a precerebellar centre providing the cerebellum with overview and integration of motor functions at systems level. A new hypothesis. J Physiol. 2013; 591:5453–8. [PubMed: 24042498]

ARBER S, LADLE DR, LIN JH, FRANK E, JESSELL TM. ETS gene Er81 controls the formation of functional connections between group Ia sensory afferents and motor neurons. Cell. 2000; 101:485–98. [PubMed: 10850491]

AVRAHAM O, HADAS Y, VALD L, ZISMAN S, SCHEJTER A, VISEL A, KLAR A. Transcriptional control of axonal guidance and sorting in dorsal interneurons by the Lim-HD proteins Lhx9 and Lhx1. Neural Dev. 2009; 4:21. [PubMed: 19545367]

BEN-ARIE N, BELLEN HJ, ARMSTRONG DL, MCCALL AE, GORDADZE PR, GUO Q, MATZUK MM, ZOGHBI HY. Math1 is essential for genesis of cerebellar granule neurons. Nature. 1997; 390:169–172. [PubMed: 9367153]

BEN-ARIE N, HASSAN BA, BERMINGHAM NA, MALICKI DM, ARMSTRONG D, MATZUK M, BELLEN HJ, ZOGHBI HY. Functional conservation of atonal and Math1 in the CNS and PNS. Development. 2000; 127:1039–48. [PubMed: 10662643]

BEN-ARIE N, MCCALL AE, BERKMAN S, EICHELE G, BELLEN HJ, ZOGHBI HY. Evolutionary conservation of sequence and expression of the bHLH protein Atonal suggests a conserved role in neurogenesis. Human Molecular Genetics. 1996; 5:1207–16. [PubMed: 8872459]

BERMINGHAM NA, HASSAN BA, WANG VY, FERNANDEZ M, BANFI S, BELLEN HJ, FRITZSCH B, ZOGHBI HY. Proprioceptor pathway development is dependent on Math1. Neuron. 2001; 30:411–22. [PubMed: 11395003]

BOSCO G, POPPELE RE. Proprioception from a spinocerebellar perspective. Physiol Rev. 2001; 81:539–68. [PubMed: 11274339]

COLE, J. Pride and a Daily Marathon. MIT Press; Cambridge, MA: 1991.

COOKE JD, LARSON B, OSCARSSON O, SJOLUND B. Origin and termination of cuneocerebellar tract. Exp Brain Res. 1971; 13:339–58. [PubMed: 5123642]

CRONE SA, QUINLAN KA, ZAGORAIOU L, DROHO S, RESTREPO CE, LUNDFALD L, ENDO T, SETLAK J, JESSELL TM, KIEHN O, SHARMA K. Genetic ablation of V2a ipsilateral interneurons disrupts left-right locomotor coordination in mammalian spinal cord. Neuron. 2008; 60:70–83. [PubMed: 18940589]

DE NOOIJ JC, DOOBAR S, JESSELL TM. Etv1 inactivation reveals proprioceptor subclasses that reflect the level of NT3 expression in muscle targets. Neuron. 2013; 77:1055–68. [PubMed: 23522042]

DING Q, JOSHI PS, XIE ZH, XIANG M, GAN L. BARHL2 transcription factor regulates the ipsilateral/contralateral subtype divergence in postmitotic dI1 neurons of the developing spinal cord. Proc Natl Acad Sci U S A. 2012; 109:1566–71. [PubMed: 22307612]

DOYLE MW, ANDRESEN MC. Reliability of monosynaptic sensory transmission in brain stem neurons in vitro. J Neurophysiol. 2001; 85:2213–23. [PubMed: 11353036]

ECCLES JC, OSCARSSON O, WILLIS WD. Synaptic action of group I and II afferent fibres of muscle on the cells of the dorsal spinocerebellar tract. J Physiol. 1961; 158:517–43. [PubMed: 13889058]

EDGLEY SA, GALLIMORE CM. The morphology and projections of dorsal horn spinocerebellar tract neurones in the cat. J Physiol. 1988; 397:99–111. [PubMed: 3411522]

EDGLEY SA, JANKOWSKA E. Information processed by dorsal horn spinocerebellar tract neurones in the cat. J Physiol. 1988; 397:81–97. [PubMed: 3411521]

FU Y, SENGUL G, PAXINOS G, WATSON C. The spinal precerebellar nuclei: calcium binding proteins and gene expression profile in the mouse. Neurosci Lett. 2012; 518:161–6. [PubMed: 22579822]

GOWAN K, HELMS AW, HUNSAKER TL, COLLISSON T, EBERT PJ, ODOM R, JOHNSON JE. Crossinhibitory activities of Ngn1 and Math1 allow specification of distinct dorsal interneurons. Neuron. 2001; 31:219–232. [PubMed: 11502254]

GRAY PA. Transcription factors define the neuroanatomical organization of the medullary reticular formation. Front Neuroanat. 2013; 7:7. [PubMed: 23717265]

HANTMAN AW, JESSELL TM. Clarke's column neurons as the focus of a corticospinal corollary circuit. Nat Neurosci. 2010; 13:1233–9. [PubMed: 20835249]

HELMS AW, ABNEY AL, BEN-ARIE N, ZOGHBI HY, JOHNSON JE. Autoregulation and multiple enhancers control Math1 expression in the developing nervous system. Development. 2000; 127:1185–96. [PubMed: 10683172]

HIPPENMEYER S, VRIESELING E, SIGRIST M, PORTMANN T, LAENGLE C, LADLE DR, ARBER S. A developmental switch in the response of DRG neurons to ETS transcription factor signaling. PLoS Biol. 2005; 3:e159. [PubMed: 15836427]

HISANO S, SAWADA K, KAWANO M, KANEMOTO M, XIONG G, MOGI K, SAKATA-HAGA H, TAKEDA J, FUKUI Y, NOGAMI H. Expression of inorganic phosphate/vesicular glutamate transporters (BNPI/VGLUT1 and DNPI/VGLUT2) in the cerebellum and precerebellar nuclei of the rat. Brain Res Mol Brain Res. 2002; 107:23–31. [PubMed: 12414120]

HUANG WH, TUPAL S, HUANG TW, WARD CS, NEUL JL, KLISCH TJ, GRAY PA, ZOGHBI HY. Atoh1 governs the migration of postmitotic neurons that shape respiratory effectiveness at birth and chemoresponsiveness in adulthood. Neuron. 2012; 75:799–809. [PubMed: 22958821]

IMONDI R, JEVINCE AR, HELMS AW, JOHNSON JE, KAPRIELIAN Z. Misexpression of L1 on pre-crossing spinal commissural axons disrupts pathfinding at the ventral midline. Mol Cell Neurosci. 2007; 36:462–71. [PubMed: 17884558]

LAI HC, KLISCH TJ, ROBERTS R, ZOGHBI HY, JOHNSON JE. In vivo neuronal subtype-specific targets of Atoh1 (Math1) in dorsal spinal cord. J Neurosci. 2011; 31:10859–71. [PubMed: 21795538]

LAKE, J.; DONAHUE, L.; DAVISSON, MT. SHIRPA assessment, C57BL/6J-Chr#A/J/NaJ mouse chromosome substitution panel. 2005. [Online]. Available: http://phenome.jax.org/db/q?rtn=projects/docstatic&doc=Lake2/Lake2_Protocol

LANDSBERG RL, AWATRAMANI RB, HUNTER NL, FARAGO AF, DIPIETRANTONIO HJ, RODRIGUEZ CI, DYMECKI SM. Hindbrain rhombic lip is comprised of discrete progenitor cell populations allocated by Pax6. Neuron. 2005; 48:933–47. [PubMed: 16364898]

LANUZA GM, GOSGNACH S, PIERANI A, JESSELL TM, GOULDING M. Genetic identification of spinal interneurons that coordinate left-right locomotor activity necessary for walking movements. Neuron. 2004; 42:375–86. [PubMed: 15134635]

LLEWELLYN-SMITH IJ, MARTIN CL, FENWICK NM, DICARLO SE, LUJAN HL, SCHREIHOFER AM. VGLUT1 and VGLUT2 innervation in autonomic regions of intact and transected rat spinal cord. J Comp Neurol. 2007; 503:741–67. [PubMed: 17570127]

LUMPKIN EA, COLLISSON T, PARAB P, OMER-ABDALLA A, HAEBERLE H, CHEN P, DOETZLHOFER A, WHITE P, GROVES A, SEGIL N, JOHNSON JE. Math1-driven GFP expression in the developing nervous system of transgenic mice. Gene Expr Patterns. 2003; 3:389–95. [PubMed: 12915300]

MACHOLD R, FISHELL G. Math1 is expressed in temporally discrete pools of cerebellar rhombic-lip neural progenitors. Neuron. 2005; 48:17–24. [PubMed: 16202705]

MADISEN L, MAO T, KOCH H, ZHUO JM, BERENYI A, FUJISAWA S, HSU YW, GARCIA AJ 3RD, GU X, ZANELLA S, KIDNEY J, GU H, MAO Y, HOOKS BM, BOYDEN ES, BUZSAKI G, RAMIREZ JM, JONES AR, SVOBODA K, HAN X, TURNER EE, ZENG H. A toolbox of Cre-dependent optogenetic transgenic mice for light-induced activation and silencing. Nat Neurosci. 2012; 15:793–802. [PubMed: 22446880]

MADISEN L, ZWINGMAN TA, SUNKIN SM, OH SW, ZARIWALA HA, GU H, NG LL, PALMITER RD, HAWRYLYCZ MJ, JONES AR, LEIN ES, ZENG H. A robust and high-throughput Cre reporting and characterization system for the whole mouse brain. Nat Neurosci. 2010; 13:133–40. [PubMed: 20023653]

MALET M, VIEYTES CA, LUNDGREN KH, SEAL RP, TOMASELLA E, SEROOGY KB, HOKFELT T, GEBHART GF, BRUMOVSKY PR. Transcript expression of vesicular glutamate transporters in lumbar dorsal root ganglia and the spinal cord of mice - Effects of peripheral axotomy or hindpaw inflammation. Neuroscience. 2013; 248:95–111. [PubMed: 23727452]

MANN MD. Axons of dorsal spinocerebellar tract which respond to activity in cutaneous receptors. J Neurophysiol. 1971; 34:1035–50. [PubMed: 4329962]

MARICICH SM, MORRISON KM, MATHES EL, BREWER BM. Rodents rely on Merkel cells for texture discrimination tasks. J Neurosci. 2012; 32:3296–300. [PubMed: 22399751]

MATEI V, PAULEY S, KAING S, ROWITCH D, BEISEL KW, MORRIS K, FENG F, JONES K, LEE J, FRITZSCH B. Smaller inner ear sensory epithelia in Neurog 1 null mice are related to earlier hair cell cycle exit. Dev Dyn. 2005; 234:633–50. [PubMed: 16145671]

MATSUSHITA M, HOSOYA Y. Cells of origin of the spinocerebellar tract in the rat, studied with the method of retrograde transport of horseradish peroxidase. Brain Res. 1979; 173:185–200. [PubMed: 90539]

MATSUSHITA M, HOSOYA Y, IKEDA M. Anatomical organization of the spinocerebellar system in the cat, as studied by retrograde transport of horseradish peroxidase. J Comp Neurol. 1979; 184:81–106. [PubMed: 84004]

MIESEGAES GR, KLISCH TJ, THALLER C, AHMAD KA, ATKINSON RC, ZOGHBI HY. Identification and subclassification of new Atoh1 derived cell populations during mouse spinal cord development. Dev Biol. 2009; 327:339–51. [PubMed: 19135992]

MIYOSHI G, HJERLING-LEFFLER J, KARAYANNIS T, SOUSA VH, BUTT SJ, BATTISTE J, JOHNSON JE, MACHOLD RP, FISHELL G. Genetic fate mapping reveals that the caudal ganglionic eminence produces a large and diverse population of superficial cortical interneurons. J Neurosci. 2010; 30:1582–94. [PubMed: 20130169]

OSCARSSON O. Functional Organization of the Spino- and Cuneocerebellar Tracts. Physiol Rev. 1965; 45:495–522. [PubMed: 14337566]

PRASAD T, WANG X, GRAY PA, WEINER JA. A differential developmental pattern of spinal interneuron apoptosis during synaptogenesis: insights from genetic analyses of the protocadherin-gamma gene cluster. Development. 2008; 135:4153–64. [PubMed: 19029045]

RAFT S, KOUNDAKJIAN EJ, QUINONES H, JAYASENA CS, GOODRICH LV, JOHNSON JE, SEGIL N, GROVES AK. Cross-regulation of Ngn1 and Math1 coordinates the production of neurons and sensory hair cells during inner ear development. Development. 2007; 134:4405–15. [PubMed: 18039969]

RANDIC M, MYSLINSKI NR, GORDON JH. Spinal localization of neurons receiving inputs from cutaneous afferents in the cat hindlimb. Brain Res. 1976; 105:573–7. [PubMed: 1260466]

ROSE MF, AHMAD KA, THALLER C, ZOGHBI HY. Excitatory neurons of the proprioceptive, interoceptive, and arousal hindbrain networks share a developmental requirement for Math1. Proc Natl Acad Sci U S A. 2009; 106:22462–7. [PubMed: 20080794]

SABA R, JOHNSON JE, SAITO T. Commissural neuron identity is specified by a homeodomain protein, Mbh1, that is directly downstream of Math1. Development. 2005; 132:2147–55. [PubMed: 15788459]

SAKAI N, INSOLERA R, SILLITOE RV, SHI SH, KAPRIELIAN Z. Axon sorting within the spinal cord marginal zone via Robo-mediated inhibition of N-cadherin controls spinocerebellar tract formation. J Neurosci. 2012; 32:15377–87. [PubMed: 23115176]

SANTARCANGELO E, POMPEIANO O, STAMPACCHIA G. Effects of kainic acid lesions of lateral reticular nucleus on posture and reflex movements. Arch Ital Biol. 1981; 119:324–40. [PubMed: 7345984]

SHERRINGTON, CS. The Integrative Action of the Nervous System. Yale University Press; New Haven, CT: 1906.

SHROYER NF, HELMRATH MA, WANG VY, ANTALFFY B, HENNING SJ, ZOGHBI HY. Intestine-specific ablation of mouse atonal homolog 1 (Math1) reveals a role in cellular homeostasis. Gastroenterology. 2007; 132:2478–88. [PubMed: 17570220]

SORIANO P. Generalized lacZ expression with the ROSA26 Cre reporter strain. Nat Genetics. 1999; 21:70–71. [PubMed: 9916792]

TALPALAR AE, BOUVIER J, BORGIUS L, FORTIN G, PIERANI A, KIEHN O. Dual-mode operation of neuronal networks involved in left-right alternation. Nature. 2013; 500:85–8. [PubMed: 23812590]

TAPPER DN, MANN MD, BROWN PB, COGDELL B. Cells of origin of the cutaneous subdivision of the dorsal spinocerebellar tract. Brain Res. 1975; 85:59–63. [PubMed: 162841]

TOURTELLOTTE WG, MILBRANDT J. Sensory ataxia and muscle spindle agenesis in mice lacking the transcription factor Egr3. Nat Genet. 1998; 20:87–91. [PubMed: 9731539]

WANG VY, ROSE MF, ZOGHBI HY. Math1 expression redefines the rhombic lip derivatives and reveals novel lineages within the brainstem and cerebellum. Neuron. 2005; 48:31–43. [PubMed: 16202707]

WATSON, C.; PAXINOS, G.; KAYALIOGLU, G. The Spinal Cord: A Christopher and Dana Reeve Foundation Text and Atlas. Academic Press; New York: 2009.

WILSON SI, SHAFER B, LEE KJ, DODD J. A molecular program for contralateral trajectory: Rig-1 control by LIM homeodomain transcription factors. Neuron. 2008; 59:413–24. [PubMed: 18701067]

YAMADA M, TERAO M, TERASHIMA T, FUJIYAMA T, KAWAGUCHI Y, NABESHIMA Y, HOSHINO M. Origin of climbing fiber neurons and their developmental dependence on Ptf1a. J Neurosci. 2007; 27:10924–34. [PubMed: 17928434]

YANG H, XIE X, DENG M, CHEN X, GAN L. Generation and characterization of Atoh1-Cre knock-in mouse line. Genesis. 2010; 48:407–13. [PubMed: 20533400]

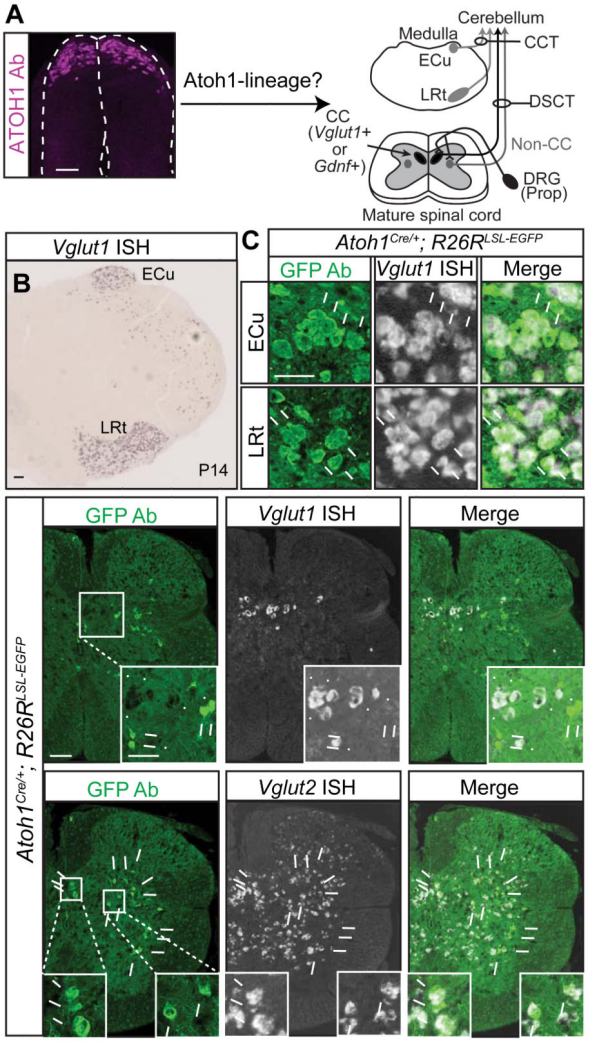

Figure 1. A majority of *Atoh1*-lineage neurons reside outside Clarke's column

(A) ATOH1 is transiently expressed in the developing neural tube (left, antibody staining). *Atoh1*-lineage neurons in the caudal rhombic lip develop into neurons of the external cuneate nucleus (ECu) in the medulla (cuneocerebellar tract, CCT, dark grey), and the lateral reticular nucleus (LRt, dark grey). In the spinal cord, it is unknown if *Atoh1*-lineage neurons contribute to Clarke's column (CC, marked by *Vglut1* or *Gdnf*, black) or non-CC (dark grey) sources of the dorsal spinocerebellar tract (DSCT). (B) *Vglut1* mRNA identifies neurons in the ECu and LRt. (C) A majority of *Atoh1*-lineage neurons (*Atoh1*$^{Cre/+}$; R26R$^{LSL\text{-}EGFP}$, GFP Ab, green) in the ECu and LRt express *Vglut1* mRNA (arrows in C, 86.7 ± 1.3% and 91.8 ± 0.2%, respectively, 3 representative sections counted per n=2 medulla from 1 litter, arrowheads for *Vglut1*+ only cells). (D) Very few *Atoh1*-lineage neurons colocalize with *Vglut1* in CC (0.5 ± 0.1%, 18 representative thoracic 5-13 (T5-13) sections per n=3 spinal cords from 2 litters, arrows for GFP+, arrowheads for *Vglut1* mRNA). (E) *Atoh1*-lineage neurons in the thoracic spinal cord are glutamatergic (82.2 ± 2.2%, 15 representative T5-13 sections per n=3 spinal cords from 2 litters, *Vglut2*+, arrows).

Mean ± SEM shown. Scale bars are 100 μm, except C and insets in D and E are 50 μm. See Figure S1 for characterization of the *Atoh1*$^{Cre/+}$ mouse.

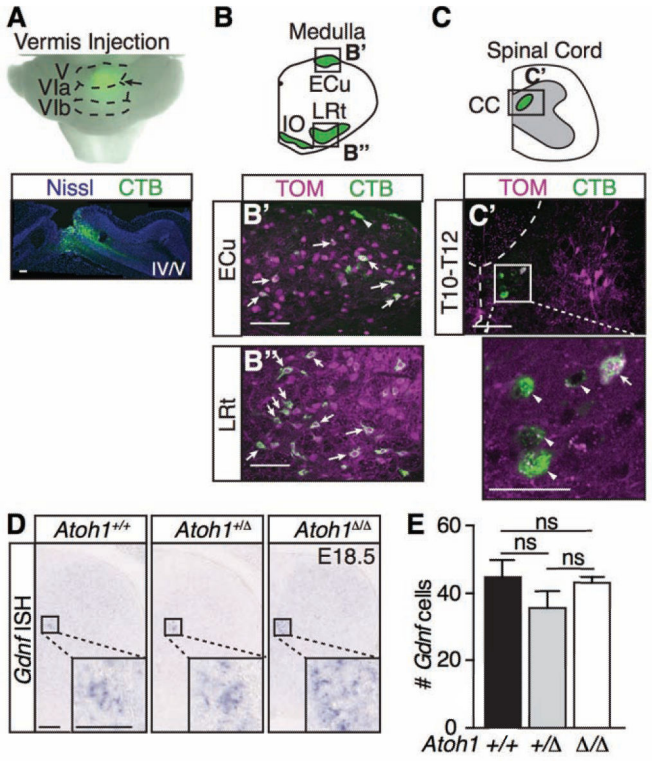

Figure 2. Clarke's column does not develop predominantly from *Atoh1*-lineage neurons

(A-C') Injection of the retrograde tracer, cholera toxin subunit B (CTB) conjugated to AlexaFluor 488 (green), into the medial area of the adult cerebellum (A, Vermis, Folia V, VIa, VIb, arrow, Nissl Neurotrace 640 in blue) results in backlabeling of cerebellar-projecting neurons in the ECu, LRt, IO (B-B''), and CC (C-C'). Several *Atoh1*-lineage neurons (TOM) in the ECu (B') and LRt (B'') colabel (arrows) with CTB. However, only 10.5 ± 0.08% of CTB+ cells in CC (C', arrowheads) colocalize with *Atoh1*-lineage neurons (arrow)(counts from 18 representative sections from T6-L3 spinal cords per n=2 mice from 2 litters). (D) *Gdnf* mRNA is unchanged in the *Atoh1* wild type ($Atoh1^{+/+}$, # Gdnf cells, 45 ± 5) versus heterozygous ($Atoh1^{+/\Delta}$, 36 ± 5) versus null mice ($Atoh1^{\Delta/\Delta}$, 43 ± 2) (p~0.2 to 0.8 in pairwise comparisons, counts from 8 representative T5-11 sections per spinal cord for each genotype, n=3 mice from 3 litters). Mean ± SEM shown. Scale bars are 100 μm and 50 μm for insets in C' and D. Abbr: external cuneate nucleus (ECu), lateral reticular nucleus (LRt), inferior olive (IO), Clarke's column (CC), not significant (ns).

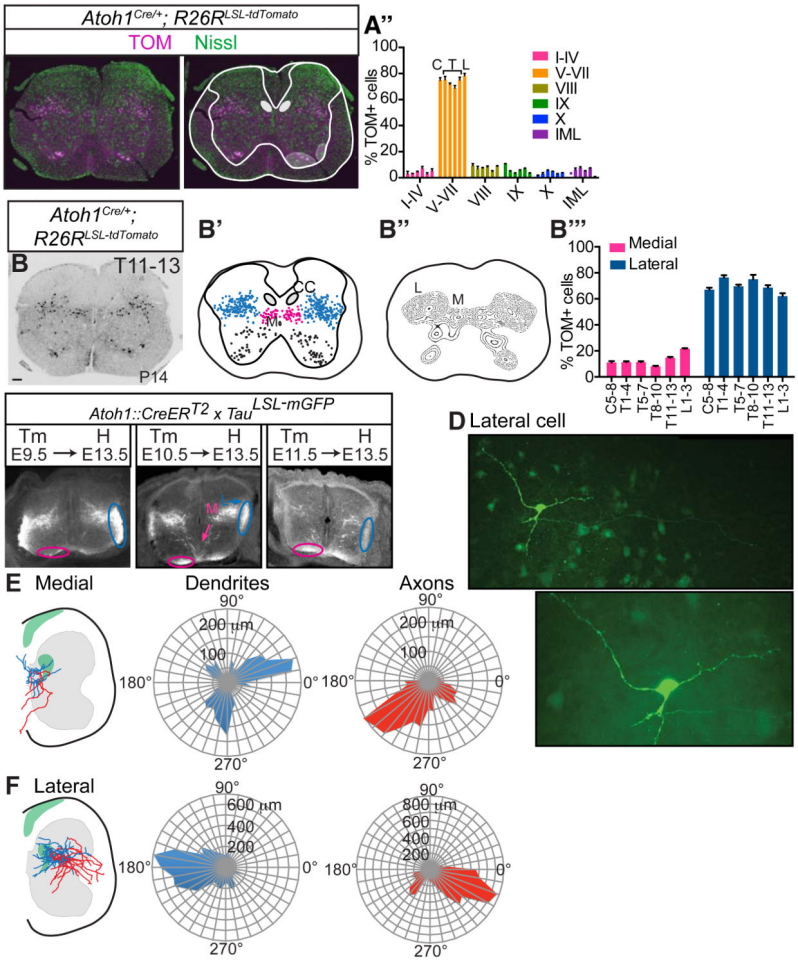

Figure 3. *Atoh1*-lineage neurons form a medial contralaterally-projecting and lateral ipsilaterally-projecting population

(A-A'') A majority of *Atoh1*-lineage neurons (TOM, magenta) reside in laminae V-VII (based on Nissl Neurotrace 488, green) throughout the rostral-caudal (r-c) axis (C, T, L bars represent C5-8, T1-4, T5-7, T8-10, T11-13, L1-3). Purple dot indicates no IML in the cervical region. (B-B'') *Atoh1*-lineage cells (TOM+, black) cluster into a medial (M, pink) and lateral (L, blue) population. (B''') Percentage of TOM+ cells in the M and L populations out of total TOM+ cells throughout the r-c axis. Six consecutive sections for one spinal cord (T11-13) stacked onto one spinal cord representation is shown in B'. Six representative sections per spinal cord region per n=3 spinal cords counted in A'' and B'''. (C) *Atoh1*-lineage neurons are born from E9.5-E11.5 where the M population (M, pink) begins projecting contralaterally to the ventral funiculus (pink oval) and the L population (L, blue) begins projecting ipsilaterally to the lateral funiculus (blue oval). (D) Example of a biocytin-stained L neuron. The axon (arrowheads) branches from a major primary neurite (arrow) and projects toward the lateral funiculus (LF). (E) M neurons have axons that project contralaterally as assayed by biocytin staining. Soma are designated as the center of the polar coordinate plot. Total dendrite (blue) and axon (red) length of a compilation of medial neurons (n=6 cells) are shown in microns (μm) on a radial axis. (F) L neurons (n=17 cells) have axons that project to the ipsilateral lateral funiculus. Green areas in E and F

indicate areas of Parvalbumin+ afferent density. Mean ± SEM shown. Scale bars are 100 μm. Abbr: Cervical (C), Thoracic (T), Lumbar (L), Clarke's column (CC), Intermediolateral Nucleus (IML). See Figure S2 for r-c data.

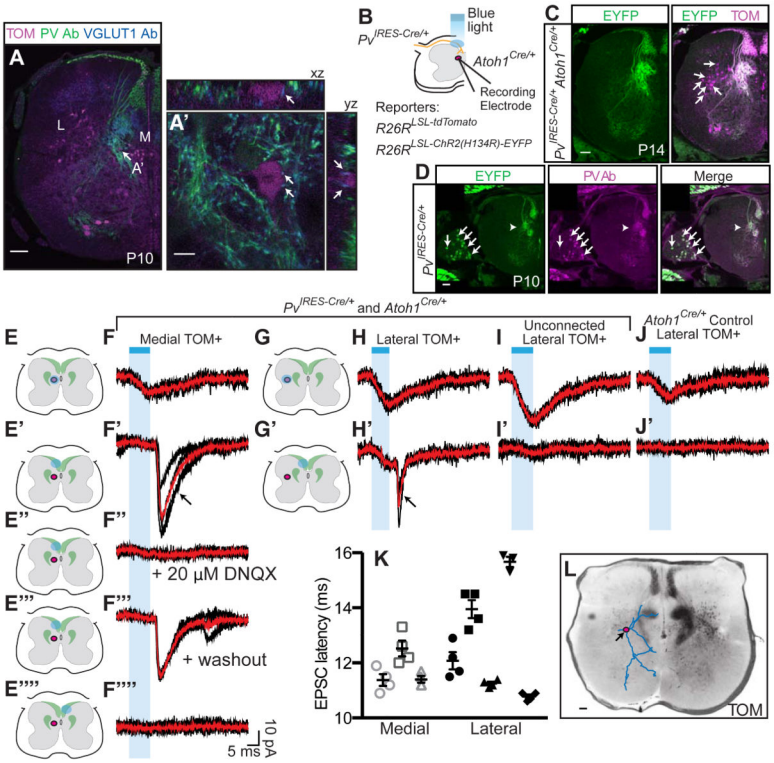

Figure 4. *Atoh1*-lineage neurons receive proprioceptive input

(A - A ') Proprioceptive afferents synapse on *Atoh1*-lineage neurons (TOM+, magenta) in the M population (Parvalbumin, PV+ (green) and VGLUT1+ (blue), arrows). (B) Proprioceptive afferents ($Pv^{IRES\text{-}Cre/+}$, yellow) and *Atoh1*-lineage neurons ($Atoh1^{Cre/+}$, magenta) express tdTomato (TOM)(Ai14) and an EYFP fused channelrhodopsin (ChR2-EYFP) (Ai32). *Atoh1*-lineage cells are recorded while focal blue light is delivered to different areas of the spinal cord slice. (C) Proprioceptive axons express both ChR2-EYFP and TOM (white), while *Atoh1*-lineage neurons have higher TOM expression (arrows, magenta). (D) Proprioceptive afferents ($Pv^{IRES\text{-}Cre/+}$) expressing ChR2-EYFP (green) colocalize with PV antibody (magenta) in the dorsal root ganglion (arrows) and axons (arrowhead). (E-F'''') Focal blue light (blue dot) delivered to a M cell (magenta oval)(E) elicits a direct inward current (F) whereas blue light delivered to the contralateral dorsal funiculus (E'''', F'''') does not. A synaptic response seen when the ipsilateral dorsal funiculus is illuminated (E', F', arrow) is blocked by DNQX (E'', F''), and recovered upon washout (E''', F'''). (G-H') A L cell has a synaptic response when the ipsilateral dorsal funiculus is illuminated (G', H', arrow). (I-J') Unconnected cells and $Atoh1^{Cre/+}$ controls have no synaptic response. Cells were held at −60 mV in voltage clamp. Three to four repeated stimulation traces are shown in black. Average trace shown in red. PV+ axons (green) are shown schematically in E-E'''' and G-G'. (K) Latency of the excitatory postsynaptic current (EPSC) is shown for 3-4 repetitions of each recorded cell: M (n=3 cells, open markers), L (n=5 cells, closed markers). Mean ± SEM shown. (L) Dendritic tree (blue processes) of a L cell that received PV+ synaptic input overlayed on TOM+ (black). Lower thoracic sections are shown. Scale bars are 100 µm except 10 µm in A'. Abbr: Medial (M), Lateral (L).

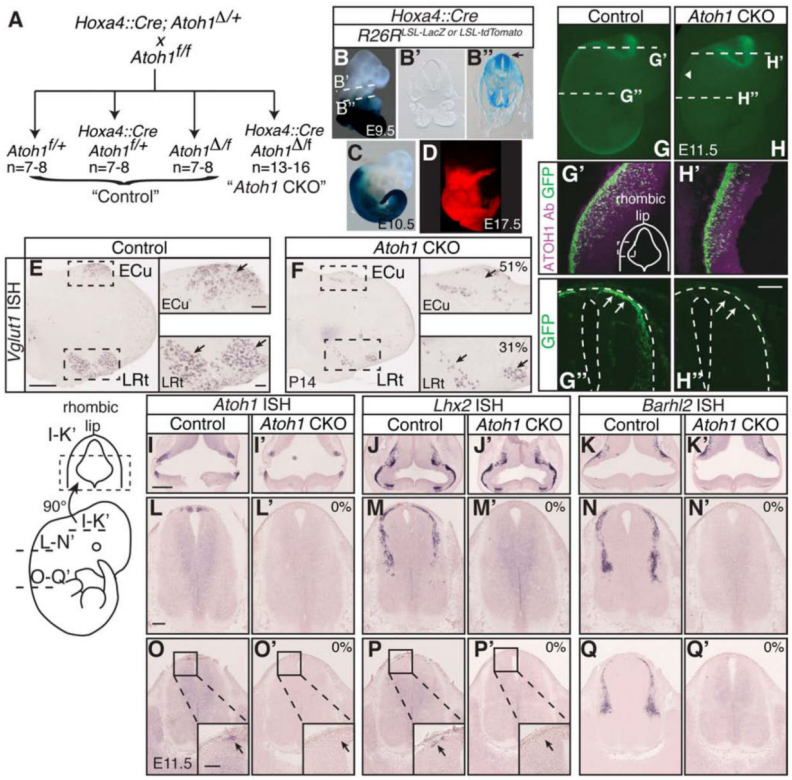

Figure 5. Conditional knock out of *Atoh1* in caudal regions of the developing neural tube

(A) Description of the cross leading to "Control" and "*Atoh1* CKO" mice. (B-D) *Hoxa4::Cre* mice express *Cre* in the caudal part of the neural tube throughout development as indicated by LacZ and tdTomato reporters (B,C,D). Cross-sections show that the LacZ reporter, reflective of *Cre* expression, is present in the *Atoh1* domain as early as E9.5 (B'', arrow). (E-F) *Vglut1*+ neurons in the ECu and LRt (arrows) are significantly reduced in *Atoh1* CKO mice (51 ± 9% *Vglut1*+ cells remaining in the ECu, 31 ± 3% in the LRt, 41 ± 5% in the total caudal medulla, mean ± SEM, 6 representative sections counted per n=3 medulla per genotype from 1 litter). (G-Q') Since ATOH1 is expressed transiently during embryogenesis, elimination of *Atoh1* and downstream markers or reporters at embryonic stages was used to assess conditional knockout efficiency. Using an *Atoh1BAC::GFP* reporter, GFP fluorescence is absent in caudal regions of the neural tube (H, arrowhead). Cross-sections show that ATOH1 (magenta) and GFP (green) are still expressed in the rhombic lip (G', H'), but GFP expression is eliminated in brachial regions of the neural tube (G'', H'')(arrows). (I-K') *Atoh1*, *Lhx2*, and *Barhl2* mRNA are present in the rhombic lip at E11.5 in control and *Atoh1* CKO embryos. (L-Q') However, at more caudal regions of the neural tube, *Atoh1*, *Lhx2*, and *Barhl2* mRNA are completely absent in the *Atoh1* CKO. Scale bars are 500 μm (E-F, I-K'), 100 μm (insets E and F, G'-H'', L-Q'), and 50 μm (insets O-P'). Abbr: external cuneate nucleus (ECu), lateral reticular nucleus (LRt).

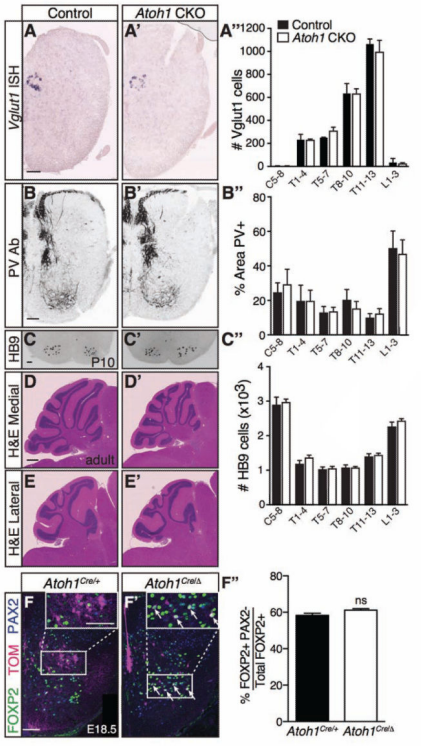

Figure 6. Neurons involved in related proprioceptive-motor pathways are unaffected in *Atoh1* CKO mice

(A-C'') Clarke's column (*Vglut1* mRNA, A-A''), proprioceptive afferents (PV Ab, B-B''), and motor neurons (HB9 Ab, C-C'') are unchanged in the *Atoh1* CKO mice at P10 (A'', B'', and C'', counts from 6 representative sections per spinal cord region for each genotype, n=3 spinal cords from 2 litters: cervical (C5-8), thoracic (T1-13), and lumbar (L1-3); control (black), *Atoh1* CKO (white); mean ± SEM). Lower thoracic sections shown. (D-E') The cerebella of control versus *Atoh1* CKO mice looks grossly normal in a hematoxylin and eosin stain of a midline sagittal section (D-D') and a lateral sagittal section (E-E'). (F-F'') A subset of *Atoh1*-lineage neurons can be detectably transfated to a FOXP2+ PAX2− population in *Atoh1* null embryos ($Atoh1^{Cre/\Delta}$, arrows). However, the percentage of FOXP2+ PAX2− cells out of total FOXP2+ cells is not significantly different (F'', counts from 8 representative T8-13 sections per n=3 spinal cords for each genotype from 2 litters, 58 ± 1% vs. 61 ± 1 %, p~0.1, mean ± SEM). Scale bar is 100 μm in A'-C', F-F', and 500 μm for D-E'.

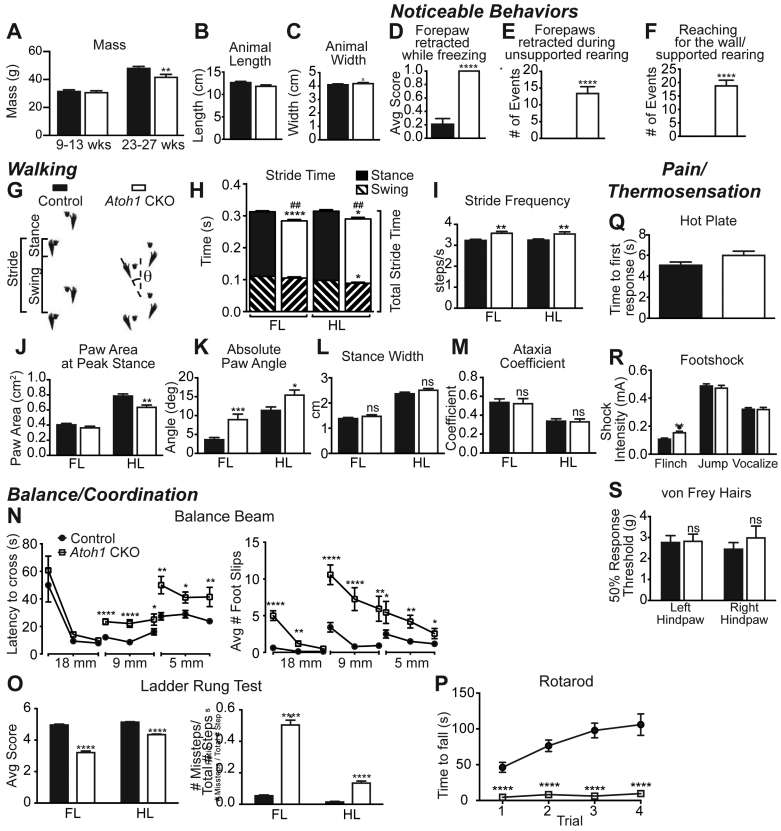

Figure 7. *Atoh1* CKO mice have balance and coordination defects

(A-C) *Atoh1* CKO mice (white) have normal mass, length, and width compared to controls (black) at 9-13 weeks old, but have less mass by 23-27 weeks. (D-F) During a five minute exposure to a novel environment, the *Atoh1* CKO mice exhibited some unique behaviors (see Movies S1 and S2). (G-M) *Atoh1* CKO mice have some walking defects. Sample footprint traces for a control and *Atoh1* CKO mouse with definitions of Swing, Stance, Stride, and Paw Angle (θ) are shown (G). *Atoh1* CKO mice have an overall decreased stride time (## $p < 0.01$) for both forelimbs (FL) and hindlimbs (HL) with a corresponding increase in stride frequency (H-I). The HL of *Atoh1* CKO mice have significantly less paw area at peak stance (J) and both FL and HL paws are pronated outward (K). *Atoh1* CKO mice have normal stance width (L) and are not ataxic (M). (N-P) *Atoh1* CKO mice have pronounced defects in balance and coordination assays. *Atoh1* CKO mice (white squares) are markedly slower and have more foot slips when crossing progressively thinner beams (18 mm, 9 mm, 5 mm) compared to control mice (black circles)(N). (O) *Atoh1* CKO mice have significantly lower quality steps on the ladder rung test and a clearly higher ratio of missteps than control for both FL and HL. See Movies S3 and S4. (P) *Atoh1* CKO mice immediately fall off an accelerating rotarod compared to control mice. (Q-S) Thermal and nociceptive responses in *Atoh1* CKO mice are normal. n=21-24 for control, n=13-16 for *Atoh1* CKO. Mean ± SEM shown. * $p < 0.05$, ** $p < 0.01$, *** $p < 0.001$, **** $p < 0.0001$. See Figure S3 for additional behaviors.